Sustainable Processes Connect
ISSN: 3079-1421
2026, Article ID. 2026.0025, Cite as: https://doi.org/10.69709/SusProc.2026.105210

SCIFINITI PUBLISHING

Research Article

OPEN ACCESS

Green Sustainable Synthesis of Silver Nanoparticles from Extracts of Garden Spearmint *Mentha spicata* for Antibiotic and Antioxidant Activities

Seyedali Mousavi[1], **Payam Ashooriyan**[1], **Mehrasa Yazdanpanah Rostami**[1], **Mahsa Erfani**[1], **Poonam Singh Nigam**[2,*]

[1] Department of Biotechnology, Faculty of Chemical Engineering, Babol Noshirvani University of Technology, Babol, Iran
[2] Biomedical Sciences Research Institute, Faculty of Life and Health Sciences, Ulster University, Coleraine BT52 1SA, UK

Article History
Received: November 25, 2025 Accepted: March 31, 2026 Published: May 21, 2026

Abstract
Silver nanoparticles (AgNPs) were synthesized via a green approach using *Mentha spicata* (*M. spicata*) extract. The extract was prepared using three methods, namely Soxhlet extraction, maceration, and ultrasonic assisted extraction, and the yields were expressed as weight percentages relative to the dry plant materia. Soxhlet extraction yielded the highest extraction efficiency at 34.36%, whereas ultrasonic assisted extraction and maceration produced yields of 18.21% and 11.80%, respectively. Although ultrasonic-assisted extraction produced a lower extraction yield, it was selected as the optimal approach due to its shorter extraction time, reduced solvent consumption, and higher energy efficiency than the other methods. The antioxidant capacity of *M. spicata* extract was notably high, with a total polyphenol content of 106.22 mg gallic acid equivalents per gram of dry plant material and an IC_{50} value of 34.02 μg/mL in the DPPH assay. Key parameters for AgNP synthesis were optimized, including pH 9, temperature of 60 °C, and extract concentration of 1.0 g/L. XRD confirmed the crystalline structure, FTIR identified functional groups, and SEM revealed an average particle size of approximately 58.41 nm. The synthesized AgNPs exhibited significant antibacterial activity against *Staphylococcus aureus*, *Proteus mirabilis*, and *Salmonella typhimurium* at the tested concentration of 5 mg/mL, highlighting the importance of optimizing extraction and synthesis conditions to enhance the bioactivity of nanoparticles.

Keywords:
green synthesis; extraction techniques; *Mentha spicata*; silver nanoparticles; antibacterial activity; antioxidant activity

1. Introduction

In recent years, metal nanoparticles have attracted considerable attention from researchers due to their physicochemical and antibacterial properties, as well as their wide range of applications [1]. Although conventional nanoparticle synthesis methods are effective, they often involve hazardous chemicals and are energy-intensive. These methods may also produce toxic by-products, which raise concerns about environmental and human health safety [2].

To address these challenges, environmentally friendly methods have been developed as practical and sustainable alternatives [2,3]. These methods employ biological agents, including plant extracts, microorganisms, and biomolecules, to convert metal ions into nanoparticles under mild reaction conditions [4]. The green synthesis of nanoparticles offers several advantages over conventional chemical methods, including reduced toxicity, lower cost, operational simplicity, and enhanced biocompatibility of the synthesized nanoparticles [5]. The synthesis of nanoparticles using herbal extracts is advantageous due to the presence of abundant bioactive compounds, including polyphenols, flavonoids, and other phytochemicals. These compounds, which are commonly found in edible culinary herbs, contribute to antiproliferative, antioxidant, and antibacterial activities [6].

* **Corresponding Author:**
Poonam Singh Nigam, Biomedical Sciences Research Institute, Faculty of Life and Health Sciences, Ulster University, Coleraine BT52 1SA, UK

Mentha is a widespread aromatic plant with a rich phytochemical composition. Four different Mentha species have demonstrated significant potential for various applications due to their antimicrobial and cytotoxic activities [7]. The high content of polyphenols and other bioactive compounds in these plant extracts facilitates efficient nanoparticle formation and imparts significant antioxidant and antimicrobial properties to the synthesized AgNPs. In previous studies, the synthesis of AgNPs using *M. spicata* extracts has been investigated and has shown promising biological activities [8]. However, a systematic comparison of extraction methods and the optimization of AgNP synthesis parameters remain limited.

In this study, an in-depth analysis of the green synthesis of AgNPs using *M. spicata* extracts was performed. Different extraction methods, including ultrasonic-assisted extraction, Soxhlet extraction, and maceration, were evaluated and compared, and key synthesis parameters, such as pH, temperature, reaction time, and extract concentration, were systematically optimized to improve nanoparticle yield and biological activity. The synthesized nanoparticles were then comprehensively characterized. In contrast to previous studies, this work systematically compares multiple extraction methods and optimizes key synthesis parameters to enhance nanoparticle yield, size uniformity, and biological activity, providing new insights into the green synthesis of *M. spicata*-mediated AgNPs.

This study aimed to comprehensively analyze the effects of extraction methods and synthesis conditions on the properties and biological activities of AgNPs synthesized using *M. spicata* extracts, with the objective of optimizing a sustainable green synthesis process for AgNPs.

2. Materials and Methods

Fresh *M. spicata* leaves were collected from the local area, and extracts were prepared using different methods, including Soxhlet extraction, ultrasonic-assisted extraction, and maceration. Unless otherwise stated, silver nitrate was obtained from Merck (Darmstadt, Germany) ($AgNO_3$, ≥99.9%), ethanol (80%, *v*/*v*), methanol, Folin–Ciocalteu reagent, gallic acid, ascorbic acid, sodium carbonate, 2,2-diphenyl-1-picrylhydrazyl (DPPH), sulfuric acid, and calcium chloride dihydrate. Gentamicin, ciprofloxacin, and sulfamethoxazole-trimethoprim were also obtained from Merck. The bacterial strains used in this study were obtained from the American Type Culture Collection (ATCC), namely *Salmonella typhimurium* (ATCC 14028), *Staphylococcus aureus* (ATCC 29213), and *Proteus mirabilis* (ATCC 12453). All chemicals and reagents used were of analytical grade and were used without further purification.

2.1. Preparation of the *M. spicata* Extract

M. spicata leaves were gathered from the outskirts of Rostam-Kola, Mazandaran Province, Iran. After being thoroughly washed, the fresh leaves were separated from stems and other plant parts with distilled water to remove dust and other impurities. To remove moisture, the leaves were air-dried for approximately one month at room temperature in a well-ventilated, shaded area. After complete drying, the leaves were ground into a fine powder using a mechanical grinder and stored in airtight containers under dry conditions until further use [9].

2.2. Extraction Methods

2.2.1. Soxhlet Extraction

A closed-end filter paper containing 15 g of dried powdered *M. spicata* leaves was placed in a Soxhlet apparatus. Extraction was performed using 300 mL of 80% ethanol under reflux conditions for 24 h [10]. The resulting extract was then filtered and stored at 4 °C until further use.

2.2.2. Maceration

A total of 1.5 g of dried powdered plant material was mixed with 30 mL of 80% ethanol, sealed tightly, and stirred continuously at 10 rpm for 24 h at room temperature, with manual shaking every 4 h [11]. After filtration, the extract was collected and stored for further use.

2.2.3. Ultrasonication

A 0.5 g sample of dried powdered plant material was mixed with 10 mL of ethanol (at concentrations of 60%, 80%, or 96%) and sonicated using a 7-mm ultrasonic probe at 70% power for durations of 4, 5, or 6 min [9]. Thereafter, the extracts were filtered and stored in airtight containers until further use.

2.3. Biosynthesis of Silver Nanoparticles (AgNPs)

For the biological synthesis of silver nanoparticles, 1.5 g of dried *M. spicata* leaf powder was subjected to ultrasonic assisted extraction using 80% ethanol. The extract was filtered through Whatman filter paper to remove solid residues and then oven-dried at 35 °C for 24 h. The dried ethanolic extract was subsequently redissolved in distilled water to a final concentration of 1 g/L, and the pH of this aqueous solution was adjusted to 9 using a calibrated pH meter, as these conditions critically influence nanoparticle formation, size, and stability [12]. A 1 mM $AgNO_3$

2026, Vol. 2, Article ID. 2026.0025
https://doi.org/10.69709/SusProc.2026.105210

solution was added dropwise to the aqueous extract under continuous stirring at 60 °C, and the reaction progress was monitored at multiple time points by measuring UV–Vis absorbance at 420 nm. After the reaction reached completion, as indicated by maximum absorbance and a visible color change, the mixture was centrifuged at 10,000 rpm for 15 min. The resulting pellet was washed three times with deionized water to remove residual ions and solvents, and subsequently oven-dried at 70 °C for 24 h. The effects of extract concentration, pH, temperature, and reaction time on AgNP synthesis were systematically evaluated to optimize the formation and stability of AgNPs.

2.4. Effect of Extract Concentration on Nanoparticle Synthesis

The effect of extract concentration on AgNP synthesis was investigated using aqueous solutions of the dried ethanolic extract at concentrations of 0.1, 0.25, 0.5, and 1 g/L [13]. For each concentration, 20 mL of the extract solution was mixed with 50 mL of 1 mM $AgNO_3$ under constant stirring at 65 °C. $AgNO_3$ solution was added gradually under constant stirring to ensure uniform reaction conditions. Absorbance at 420 nm was measured using a spectrophotometer at 15, 30, 60, and 1440 min [13].

2.5. Effect of Temperature

The effect of temperature on AgNP synthesis was investigated at room temperature and at 50, 60, and 70 °C using an aqueous solution of the dried extract (1 g/L) at the optimized pH of 9. Absorbance was measured at 420 nm. Temperature plays a crucial role in controlling nucleation and growth rates; higher temperatures accelerate the reduction of silver ions but may also increase particle size due to aggregation. Therefore, precise temperature control is essential to achieve the desired nanoparticle properties [9].

2.6. Effect of pH

The optimized concentration of dried ethanolic extract (1 g/L) was dissolved in distilled water, and the pH of the solution was adjusted to 6, 7, 8, and 9 using a calibrated pH meter. A 1 mM $AgNO_3$ solution was then added to the aqueous extract, and the reaction was carried out at 60 °C under magnetic stirring. The absorbance of the samples was measured at 420 nm. The sample showing the highest absorbance value was selected for subsequent experiments [14].

2.7. Influence of Reaction Duration

An extract concentration of 1 g/L and a 1 mM silver nitrate solution were prepared to investigate the effect of reaction time [13,15], with the pH adjusted to 9 using distilled water. The formation of silver nanoparticles was observed while the mixture was maintained at 60 °C under constant stirring. Absorbance measurements at 420 nm were recorded at 15, 30, 60, and 1440 min to monitor the progression of nanoparticle synthesis.

2.8. Collection and Purification of AgNPs

The reaction mixture exhibiting the highest absorbance under optimized conditions of extract concentration, pH, and temperature was collected for nanoparticle purification. The AgNPs were centrifuged at 10,000 rpm for 15 min, and the resulting precipitate was washed three times with deionized water to remove residual ethanol and unreacted silver ions. The purified nanoparticles were then oven-dried at 70 °C for 24 h and stored for subsequent characterization using SEM, XRD, and FTIR. This procedure was performed to remove residual solvents and reactants, thereby yielding reproducible samples suitable for physicochemical and biological analyses.

2.9. Characterization of Silver Nanoparticles

2.9.1. UV-Visible Spectroscopy

UV–Vis spectroscopy was conducted using a Shimadzu spectrophotometer over a wavelength range of 220–620 nm to evaluate the optical properties of the synthesized AgNPs. The formation of nanoparticles was confirmed by the presence of a characteristic surface plasmon resonance (SPR) peak. Absorbance values were recorded directly without normalization [16,17].

2.9.2. Functional Group Identification

Functional groups present in the *M. spicata* extract that contribute to the reduction and stabilization of silver ions were identified using Fourier-transform Infrared (FTIR) spectroscopy analysis [18].

2.9.3. X-ray Diffraction (XRD)

The crystalline structure and phase purity of the synthesized AgNPs were examined using X-ray diffraction (XRD) analysis with Cu Kα radiation, confirming a face-centered cubic crystalline phase characteristic of silver nanoparticles [19].

2.9.4. Morphological Analysis

The size and morphology of the synthesized AgNPs were examined using scanning electron microscopy (SEM) analysis [20].

2.9.5. Antioxidant Activity

The Folin–Ciocalteu colorimetric method was used to determine the total phenolic content (TPC) of *M. spicata* leaves [21]. Whatman No. was used to filter the mixture. Before being used in further biochemical analyses, the filtrate was oven dried at 35 °C for 24 h using filter paper. A 1000 ppm stock solution of gallic acid was prepared in 70% methanol, and standard solutions of 12.5, 25, 50, and 100 ppm were prepared for the construction of a calibration curve. A 0.5 mL aliquot of the solution was mixed with 2.5 mL of 0.5 M Folin–Ciocalteu reagent for both standards and samples. After 5 min, 2 mL of 7.5% sodium carbonate was added. After incubation in the dark at room temperature for 30 min, the absorbance of the mixture was measured at 720 nm. A gallic acid calibration curve was used to calculate total phenolic content (TPC), which was expressed as mg GAE/g dry extract [21].

2.10. Antibacterial Activity of Synthesized Nanoparticles

2.10.1. Disc Diffusion Method

Following the Kirby–Bauer procedure (2009) [22], the antibacterial efficacy of *M. spicata* extracts and biosynthesized AgNPs was evaluated using the disc diffusion method, with the pH adjusted to 7.2–7.4. Three common bacterial strains were tested: *S. typhimurium* (ATCC 14028), *Proteus mirabilis* (ATCC 12453), and *Staphylococcus aureus* (ATCC 29213). Bacterial suspensions prepared from 24-h cultures on blood agar were adjusted to the 0.5 McFarland standard using sterile saline. Using sterile forceps, sterile discs containing 20 µL of either AgNPs (0.1–5 mg/mL) or plant extract (2.5–25 mg/mL) were placed on the agar surface. Antibiotic discs containing gentamicin, ciprofloxacin, and sulfamethoxazole-trimethoprim were placed on the plates as positive controls. The plates were incubated at 37 °C for 24 h. After incubation, the zones of inhibition were measured to evaluate antimicrobial activity.

2.10.2. Tube Dilution Screening (Qualitative)

A preliminary tube dilution assay was performed to determine the effective concentration range of the biosynthesized AgNPs for subsequent disc diffusion testing. Serial twofold dilutions of AgNP suspensions (0.1–5 mg/mL) were prepared in nutrient broth and incubated with test microorganisms. This assay was used only as a qualitative screening to select concentrations for disc diffusion assays; formal minimum inhibitory concentration (MIC) and minimum bactericidal concentration (MBC) determinations were not conducted in the present study.

3. Results and Discussion

3.1. The Extraction Efficiency of *M. spicata* Plants

Three methods were employed to evaluate the extraction efficiency of *M. spicata* leaves, namely Soxhlet extraction, maceration, and ultrasonic-assisted extraction. Soxhlet extraction was the most effective of the traditional techniques, producing 0.3436 g of extract per gram of dry plant material after 24 h. In contrast, under the same circumstances, maceration showed a much lower extraction efficiency of 0.1180 g extract/g dry plant material. Different combinations of extraction times (4, 5, and 6 min) and ethanol concentrations (60%, 80%, and 96%) were tested to optimize the ultrasonic extraction process. Table 1 presents a comparative overview of the extraction methods employed in this study. The extraction efficiency of *M. spicata* using the ultrasonic method is shown in Table 2. The highest extraction yield was obtained using 80% ethanol with a sonication time of 6 min. This was identified as the optimal condition for further studies. Although ultrasonic-assisted extraction yielded a slightly lower extract yield compared with Soxhlet extraction, it was selected as the preferred method due to its significantly lower energy consumption, reduced solvent usage, shorter extraction time, and overall sustainability benefits.

3.2. The Green Synthesis of Silver Nanoparticles

3.2.1. Effect of Extract Concentration

The concentration of *M. spicata* extract significantly influenced the formation of AgNPs [23]. A rapid and pronounced color change from light brown to deep brown within 1 h indicated that higher extract concentrations accelerated the reaction [23,24]. This visible color change is typically attributed to the surface plasmon resonance phenomenon and is commonly used as an indicator of AgNP formation [17].

2026, Vol. 2, Article ID. 2026.0025
https://doi.org/10.69709/SusProc.2026.105210

As shown in Figure 1, enhanced nanoparticle formation was confirmed by an increase in absorbance at 420 nm at higher extract concentrations. Across all time points (15, 30, 60, and 1440 min), the 1 g/L concentration exhibited the highest absorbance values, indicating the most rapid and efficient synthesis of AgNPs [25]. In contrast, lower concentrations (0.1, 0.25, and 0.5 g/L), displayed slower reaction rates, lower yields, less noticeable color changes, and lower absorbance values [26].

Increased extract concentrations enhanced nanoparticle synthesis, which can be attributed to the greater availability of phytochemicals such as polyphenols and flavonoids. Vanlalveni et al. [12] reported that these bioactive constituents act as natural reducing and stabilizing agents during the synthesis process [12]. These results are consistent with the findings of Ghosh et al. [27], who reported that increasing plant extract concentration accelerates the reduction of silver ions, thereby enhancing nanoparticle production and improving control over particle size. Accordingly, an extract concentration of 1 g/L was selected as the optimal condition for subsequent experimental procedures.

Table 1: Comparative summary of the extraction methods and their effects on AgNP synthesis.

Extraction Method	Extraction Time	Solvent Consumption	Relative Extraction Yield	AgNP Formation Efficiency
Soxhlet extraction	Long	High	High	Moderate
Maceration	Very long	Moderate	Moderate	Low-moderate
Ultrasonic-assisted extraction	Short	Low	High	High

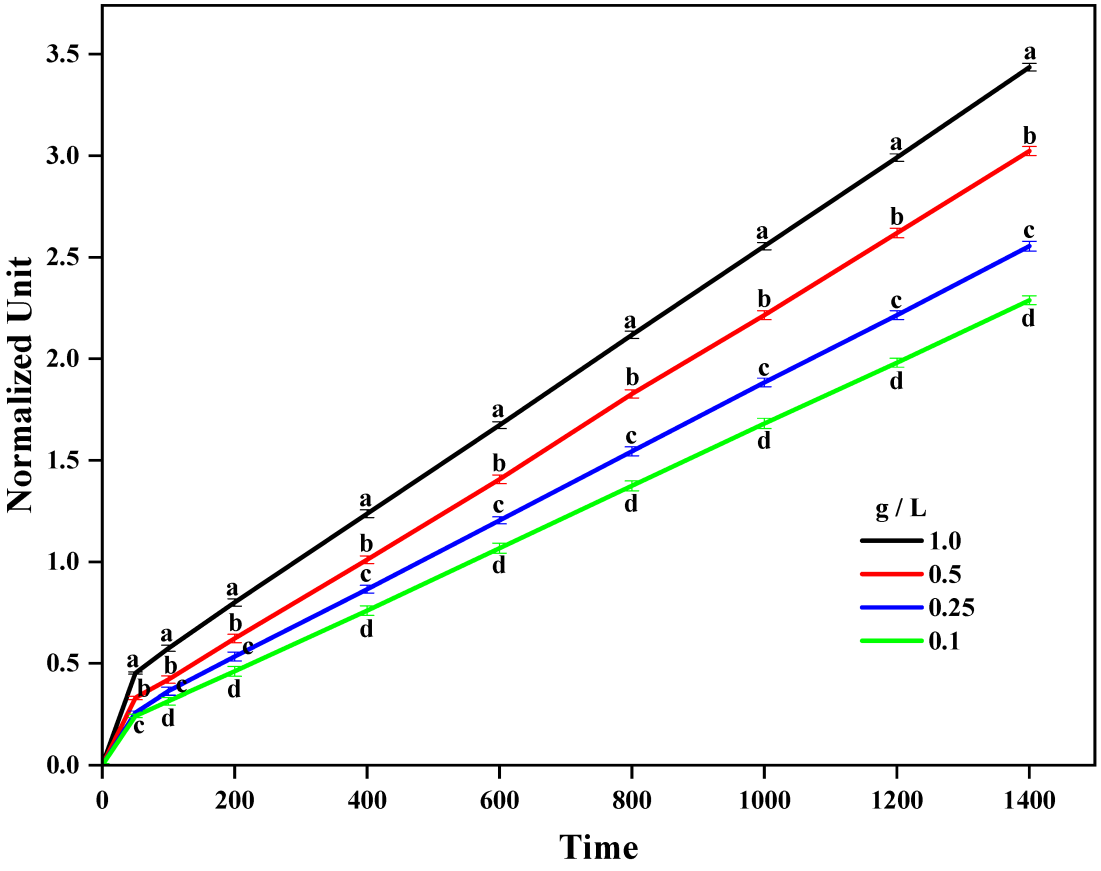

Figure 1: Effect of extract concentration on AgNP synthesis at different time points. Data are shown as mean ± SD (n = 3). Different superscript letters (a–d) indicate statistically significant differences at each time point, determined by one-way ANOVA followed by Tukey's test using SPSS ($p < 0.05$).

2026, Vol. 2, Article ID. 2026.0025
https://doi.org/10.69709/SusProc.2026.105210

Table 2: Extraction efficiency of *M. spicata* plants by the ultrasonic method.

Method	Dry Weight of the Plant (g)	Time (min)	Ethanol (%)	Extraction Yield (%, *w*/*w*, Based on Dry Plant Mass)
Ultrasonic method	0.5	4	60	2.1673 ± 0.2 [h]
			80	4.7766 ± 0.3 [g]
			96	0.9759 ± 0.06 [i]
	0.5	5	60	16.9298 ± 0.3 [c]
			80	17.2846 ± 0.2 [b]
			96	9.5371 ± 0.4 [f]
	0.5	6	60	12.0775 ± 0.3 [d]
			80	18.2090 ± 0.5 [a]
			96	10.8270 ± 0.4 [e]

Results are expressed as mean ± standard deviation (SD) (n = 3). Statistical analysis was performed using one-way analysis of variance (ANOVA) followed by Tukey's post hoc test in SPSS software. Differences were considered statistically significant at $p < 0.05$. Mean values within the same column with different superscript letters(a–i) indicate significant differences.

3.2.2. Effect of pH

The synthesis of AgNPs was significantly influenced by the pH of the reaction mixture. Alkaline conditions promote the reduction of silver ions, as evidenced by an increased rate of AgNP formation with rising pH levels [28]. Elevated pH levels accelerate nanoparticle formation by increasing the ionization of phytochemicals in the extract, particularly phenolic compounds, thereby enhancing their reducing potential [29]. The fastest and most efficient synthesis occurred at pH 9 with an extract concentration of 1 g/L and a reaction temperature of 60 °C. Because pH 9 was identified as optimal for nanoparticle formation, it was selected for further experiments. Figure 2 illustrates the visual color changes of the reaction mixture and the corresponding UV–Vis absorbance spectra at different pH levels, confirming enhanced nanoparticle formation under alkaline conditions.

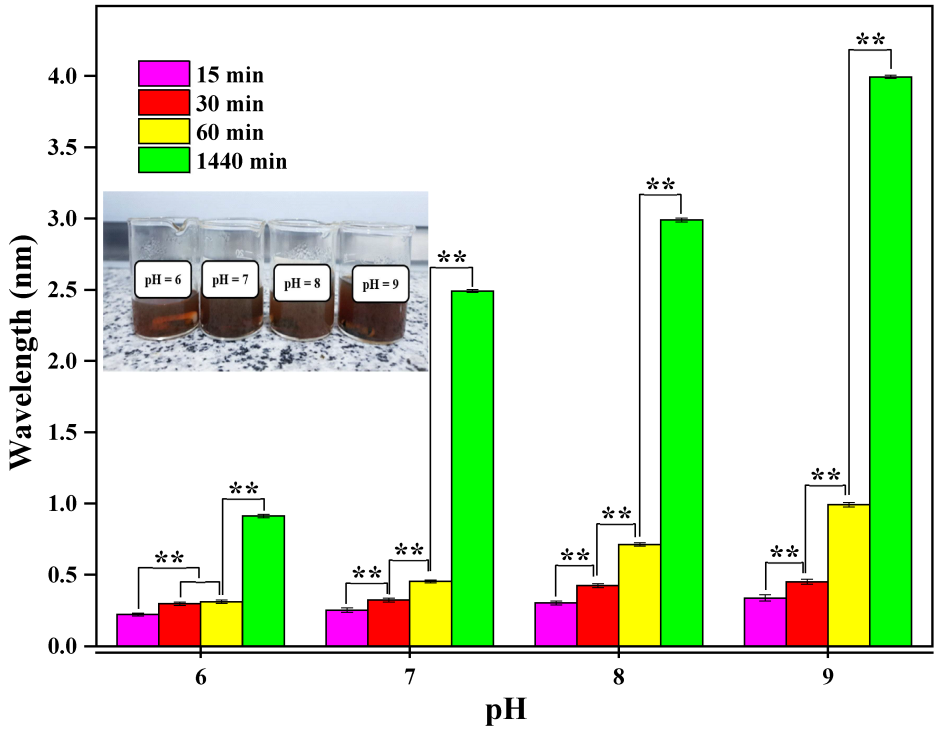

Figure 2: Effect of pH on the synthesis of AgNPs. The graph shows the variation in nanoparticle formation at different pH values. ** indicates statistically significant differences between groups ($p < 0.05$).

2026, Vol. 2, Article ID. 2026.0025
https://doi.org/10.69709/SusProc.2026.105210

3.2.3. Effect of Temperature

The rate and efficiency of AgNP synthesis were significantly influenced by temperature [30]. Increasing the temperature reduced the time required for nanoparticle formation by accelerating the reduction of silver ions [31,32]. The increased molecular kinetics and reactivity at higher temperatures are consistent with this inverse relationship between temperature and synthesis time [32]. AgNP formation was observed at 25 °C, 50 °C, 60 °C, and 70 °C at a fixed extract concentration of 1 g/L. As shown in Figure 3, at 25 °C, the reaction took approximately 10 h; at 50 °C and 60 °C, the reaction times decreased to 5 h and 30 min, respectively. Although the reaction rate increased slightly at 70 °C, extended exposure resulted in nanoparticle agglomeration. Thus, 60 °C was determined to be the optimal temperature for producing consistent and stable nanoparticles.

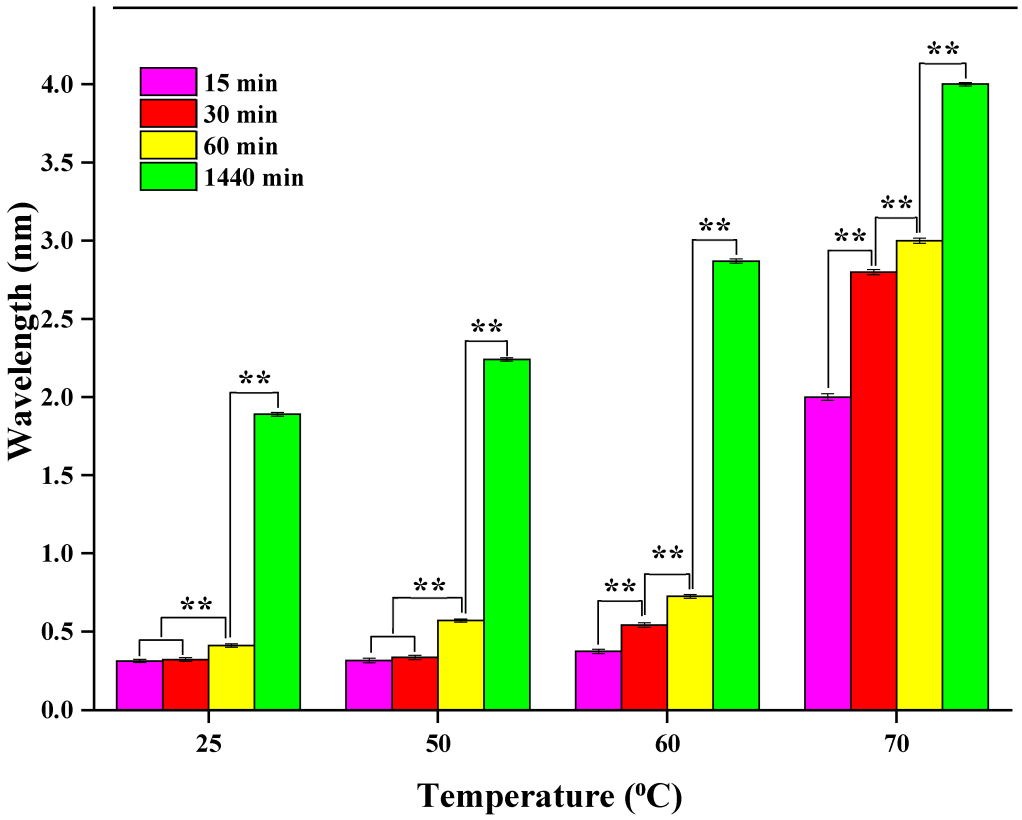

Figure 3: Effect of temperature on the synthesis of AgNPs. The graph shows the variation in nanoparticle formation at different temperatures. ** indicate statistically significant differences between groups ($p < 0.05$).

Silver nanoparticle nucleation and growth were observed within 30 min, with initial changes evident as early as 10 min. These results indicate that higher temperatures accelerate nanoparticle formation while maintaining stability under optimal conditions [33].

3.3. Characterization of the Synthesized Silver Nanoparticles

3.3.1. UV-Vis Spectral Analysis

UV–Vis spectra recorded over the wavelength range of 220–620 nm revealed a distinct surface plasmon resonance (SPR) band, confirming the successful synthesis of AgNPs [34]. This characteristic absorption peak arises from the collective oscillation of conduction electrons on the nanoparticle surface upon excitation by incident light, a phenomenon known as localized surface plasmon resonance (LSPR) [35]. The prominent and distinct SPR peak at $\lambda max \approx 420$ nm, shown in Figure 4, verifies the successful synthesis of AgNPs with a relatively uniform particle size distribution [36]. Furthermore, this peak serves as a reliable indicator of nanoparticle formation and stability, as its position, intensity, and shape are influenced by factors such as particle size, morphology, concentration, and

the surrounding medium, in agreement with previously reported studies on AgNPs [37].

3.3.2. FTIR Analysis

The FTIR spectra of *M. spicata* extract combined with $AgNO_3$ were recorded over the 400–4000 cm^{-1} range, as shown in Figure 5. The spectra indicate the presence of various functional groups and phytochemical constituents that may participate in the biosynthesis of silver nanoparticles. Phytochemical analysis of the extract in the presence of $AgNO_3$ suggests the presence of bioactive compounds, including phenolic and flavonoid-related functional groups, which are commonly reported to contribute to nanoparticle formation [38,39]. The spectrum, therefore, reflects the interaction between Ag+ ions and plant-derived biomolecules rather than confirming specific molecular identities [40].

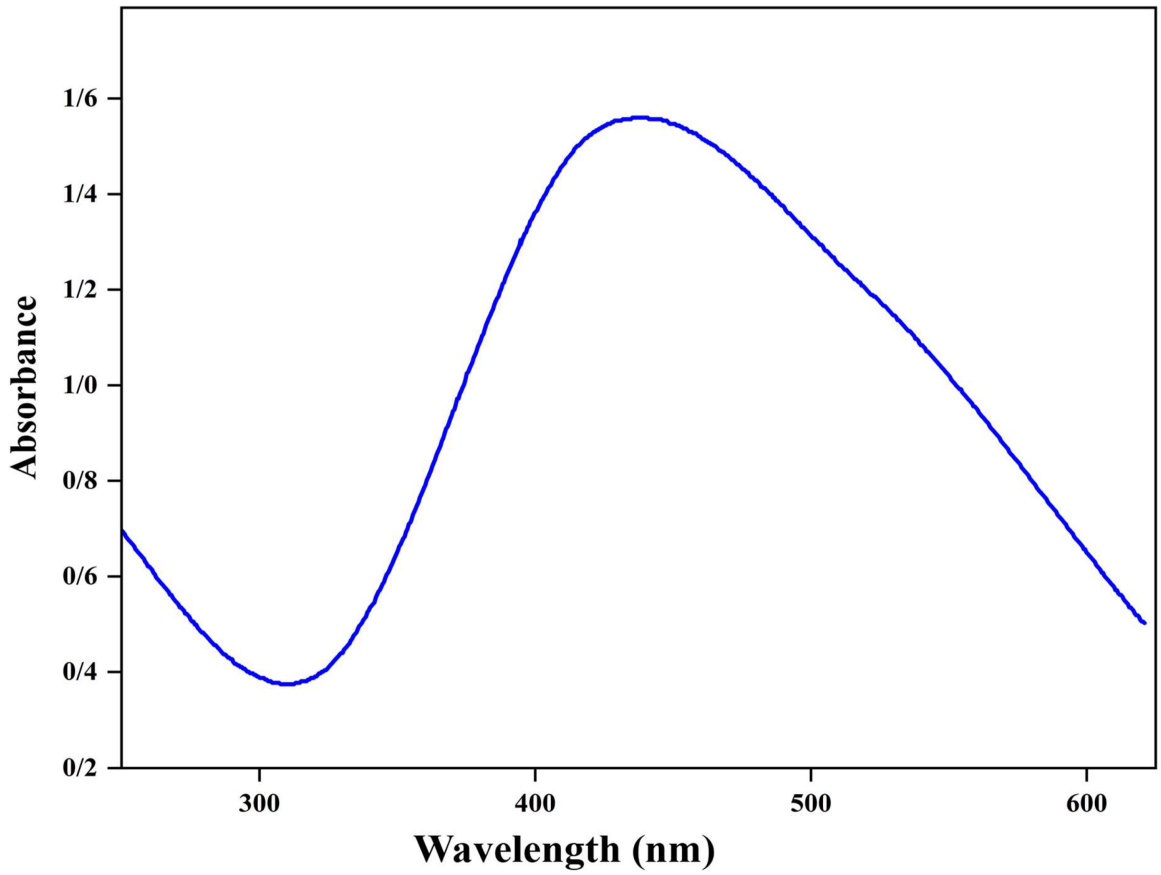

Figure 4: UV–Vis spectrum of AgNPs synthesized using *M. spicata* extract over the wavelength range 220–620 nm; showing a prominent SPR peak at λmax ≈ 420 nm.

The FTIR spectra presented in Figure 5 compare the synthesized AgNPs with the ethanolic extract of *M. spicata* leaves. A broad absorption band around 3423 cm^{-1} observed in the leaf extract is attributed to the stretching vibrations of hydroxyl (-OH) groups, commonly found in alcohols and phenols [41]. A shift from 2977 cm^{-1} to 2898 cm^{-1} was noted, corresponding to C–H stretching vibrations typical of aliphatic compounds [42]. The peak at 1647 cm^{-1} is attributed to carbonyl (C=O) stretching vibrations, whereas the band at 1047 cm^{-1} corresponds to C–O functional groups [18]. Furthermore, the signal near 1452 cm^{-1} may be attributed to C–N stretching vibrations in aliphatic amines [18,38,41].

2026, Vol. 2, Article ID. 2026.0025
https://doi.org/10.69709/SusProc.2026.105210

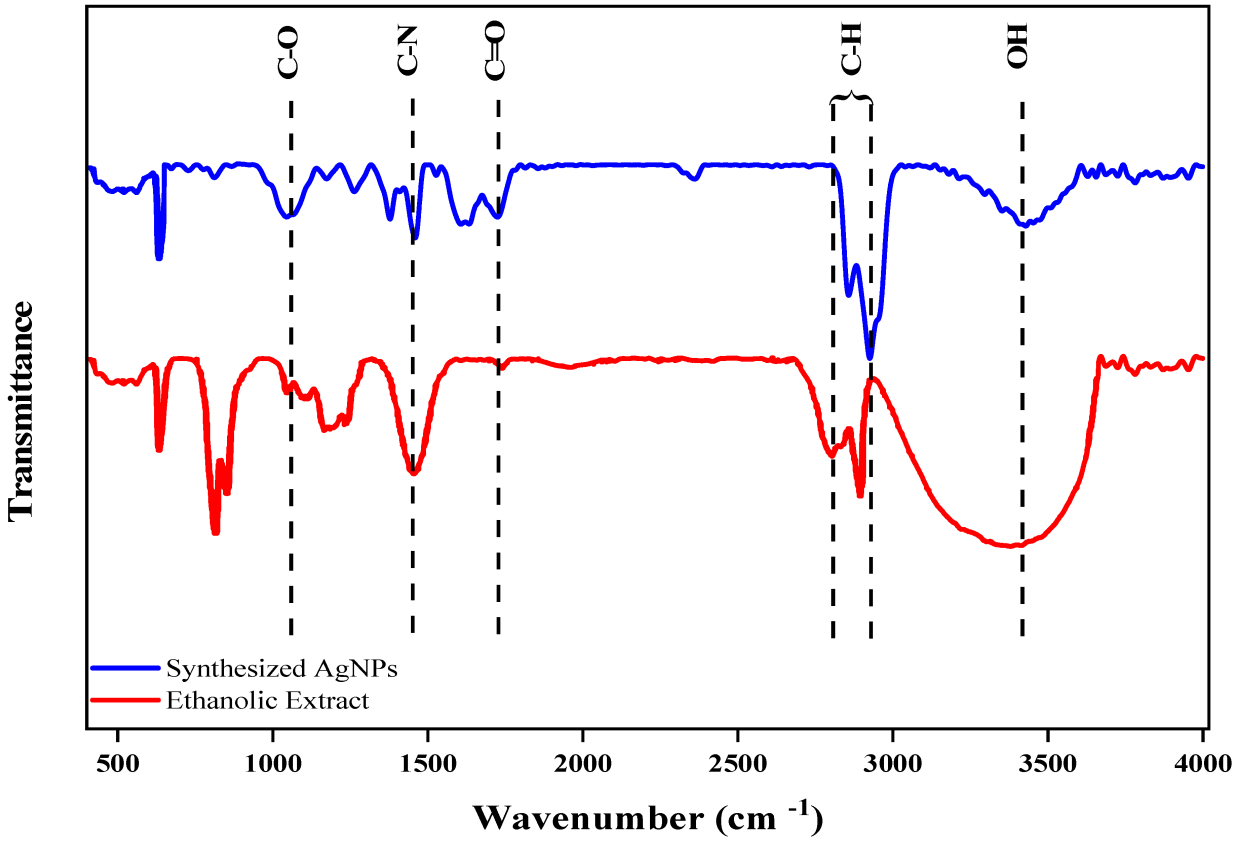

Figure 5: FTIR spectra of (a, red) the ethanolic extract of *M. spicata* and (b, blue) the synthesized AgNPs.

In the spectrum of the synthesized AgNPs, the -OH absorption shifted slightly to 3427 cm^{-1}, and C–H stretching bands moved from 2856 cm^{-1} to 2925 cm^{-1} [24]. Peaks observed in the 1173–1262 cm^{-1} region are typically attributed to C–O stretching vibrations, which are commonly associated with polyphenolic and flavonoid-containing compounds. In addition, carbonyl-related absorption bands were observed in the range of 1606–1724 cm^{-1} [43]. The band detected at approximately 1458 cm^{-1} can be associated with C–N stretching vibrations of aliphatic amine groups [18,41].

Comparison of the two spectra reveals noticeable shifts in several absorption bands, indicating possible interactions between silver ions and plant-derived functional groups during nanoparticle formation [44]. The shift in the –OH stretching frequency from 3423 to 3427 cm^{-1} suggests the involvement of hydroxyl-containing compounds, such as phenolics and alcohols, in the reduction and stabilization of the nanoparticles [24].

Overall, the FTIR results suggest that polyphenolic compounds, including flavonoids present in *M. spicata*, may contribute to the reduction and capping of silver nanoparticles. However, FTIR analysis alone does not enable definitive identification of the specific phytochemicals involved, and the proposed roles are inferred based on functional group interactions commonly reported in plant-mediated nanoparticle synthesis [24].

3.3.3. XRD Analysis

X-ray diffraction (XRD) analysis was employed to examine the crystalline structure of AgNPs synthesized using *M. spicata* extract [24]. The diffraction pattern displayed in Figure 6 shows prominent peaks at 2θ = 37.95°, 44.45°, 64.45°, and 77.35°, corresponding to the (111), (200), (220), and (311) planes of face-centered cubic (fcc) metallic silver [24]. The appearance of these characteristic peaks confirms that crystalline AgNPs were successfully synthesized, as the diffraction angles match those listed in the standard JCPDS card no. 04-0783.

The average crystallite size (D) of the AgNPs was calculated using the Scherrer equation applied to the (111) diffraction peak, yielding an approximate value of 13 nm. This value represents the size of the crystalline core of the nanoparticles. Furthermore, the sharpness and intensity of the diffraction peaks reflect the high crystallinity of the

synthesized AgNPs, supporting their crystalline formation and structural stability [45].

3.3.4. SEM Analysis

The morphology and size characteristics of the biosynthesized silver nanoparticles were investigated using scanning electron microscopy (SEM) [24]. This technique employs a focused electron beam to generate high-resolution images of the sample surface, enabling detailed visualization of particle shape and size distribution [46]. SEM micrographs of AgNPs synthesized under optimized conditions are shown in Figure 7. Image analysis indicated that the majority of nanoparticles exhibited a nearly spherical morphology with an average diameter of approximately 58.41 nm [41]. This measured size is larger than the crystallite size obtained from XRD (~13 nm), which represents only the crystalline core of the nanoparticles. The observed difference is attributed to the presence of a stabilizing layer and possible particle aggregation, while the consistent size and shape across the sample confirm that the green synthesis method produced nanoparticles with relatively uniform morphology.

Overall, the combined XRD and SEM analyses provide complementary insights, with XRD confirming the crystalline nature and core size of the nanoparticles, while SEM elucidates their overall size, morphology, and uniformity. Together, these results support the reliability of nanoparticle characterization and the reproducibility of the synthesis process [47].

3.3.5. Antioxidant Activity of the *M. spicata* Plant

The antioxidant activity of *M. spicata* was evaluated by determining the total phenolic content of the ethanolic extract used for silver nanoparticle synthesis. This was determined using the Folin–Ciocalteu method. The total phenolic content was 106.22 mg gallic acid equivalents (GAE) per gram of dried plant material [48]. The DPPH assay was used to evaluate the antioxidant capacity of the extract by measuring its free radical-scavenging activity [49]. The concentration required to achieve 50% inhibition (IC_{50}) for the *M. spicata* extract was determined to be 34.0217 µg/mL, indicating moderate antioxidant activity, in comparison with vitamin C, which exhibited an IC_{50} value of 8.86 µg/mL [50]. The inhibition curve illustrating the extract's antioxidant activity is shown in Figure 8 [49]. These results demonstrate that *M. spicata* exhibits appreciable free-radical-scavenging capacity, where a lower IC_{50} value corresponds to stronger antioxidant activity [48].

3.4. Antibacterial Activity of Synthesized Nanoparticles

3.4.1. Disc Diffusion Method

AgNPs synthesized using *M. spicata* leaf extract exhibited significant antibacterial activity, particularly at higher concentrations [24,51]. The inhibitory effect of AgNPs on bacterial growth was concentration-dependent [51,52]. As the concentration of the AgNP solution decreased, the inhibitory effect decreased correspondingly [53]. Figure 9 illustrates the antibacterial activity by comparing the zones of inhibition produced by the synthesized AgNPs (panel A) with those produced by standard antibiotic controls (panel B) against the tested bacterial strains. The presence of clear zones surrounding the discs demonstrates the strong antibacterial activity exhibited by the AgNPs biosynthesized from *M. spicata* [17,54].

3.4.2. Tube Dilution Method

To evaluate microbial growth inhibition, AgNPs synthesized using the optimized ultrasonic extract were tested. Table 3 presents the inhibitory effects of AgNPs at concentrations of 5, 1, 0.5, 0.25, and 0.1 mg/mL, demonstrating a clear dose-dependent response comparable to that of standard antibiotics. The AgNPs exhibited the highest antibacterial activity against *Staphylococcus aureus*, while the lowest activity was observed against *Salmonella typhimurium* [54]. The data indicate that while the *M. spicata* plant extract alone showed no significant antibacterial activity against the tested bacterial strains, the AgNPs synthesized from the extract effectively inhibited bacterial growth [51,55,56]. The preliminary screening using the tube dilution method was performed to identify the effective concentration range of the synthesized AgNPs. Based on these observations, a concentration range of 0.1 to 5 mg/mL was selected for detailed evaluation using the disc diffusion assay. The results of the tube dilution assay were consistent with the inhibition zones reported in Table 3, confirming the dose-dependent antibacterial activity.

2026, Vol. 2, Article ID. 2026.0025
https://doi.org/10.69709/SusProc.2026.105210

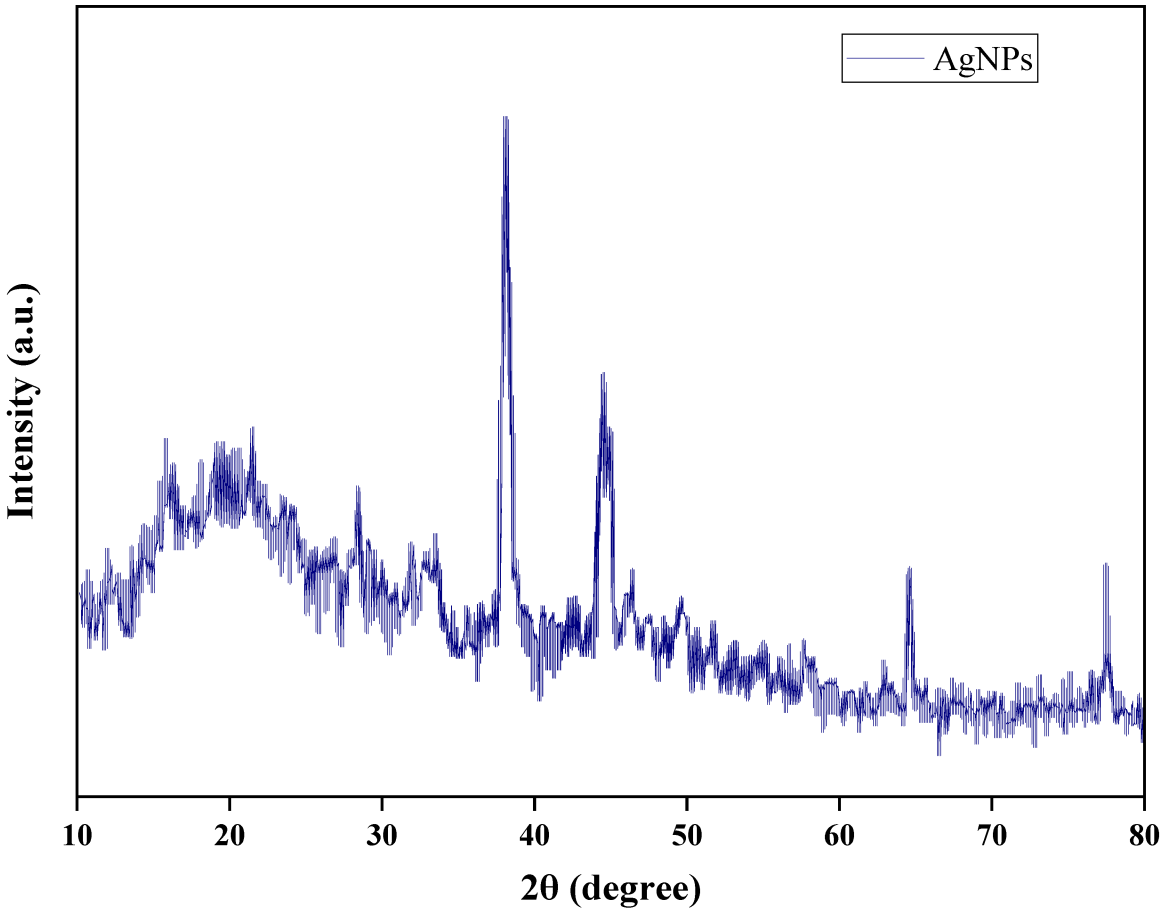

Figure 6: XRD pattern of AgNPs.

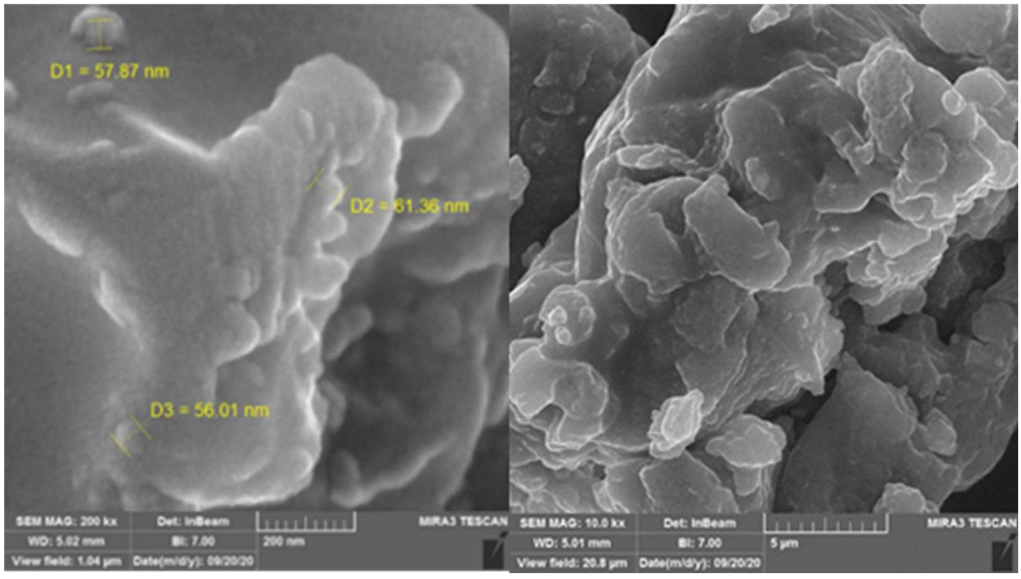

Figure 7: Scanning electron microscopy image showing the morphology and dimensional properties of biosynthesized silver nanoparticles, showing a roughly spherical shape with an average diameter of approximately 58.41 nm (diameters D1 = 57.87, D2 = 61.36, and D3= 56.01 nm, shown in yellow on the micrograph).

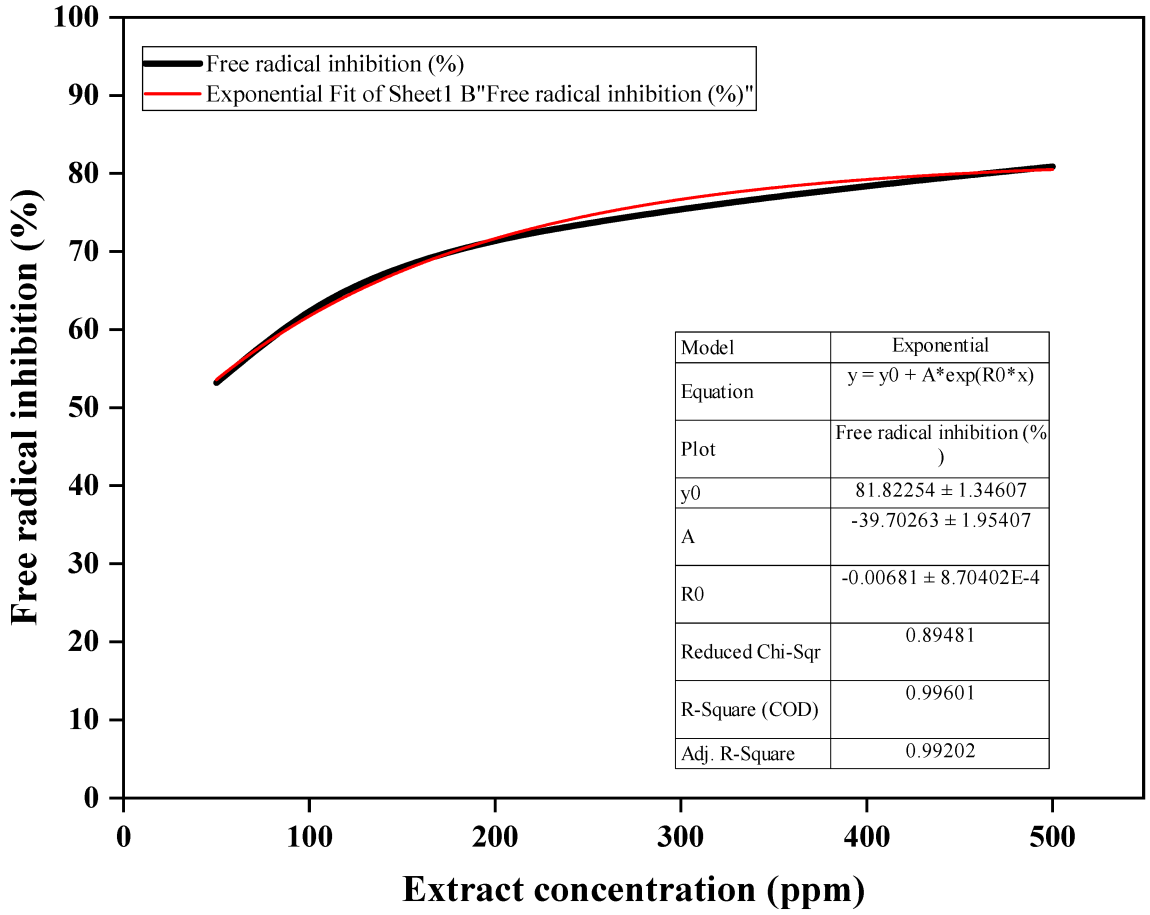

Figure 8: Inhibition of free radicals by *M. spicata* extract.

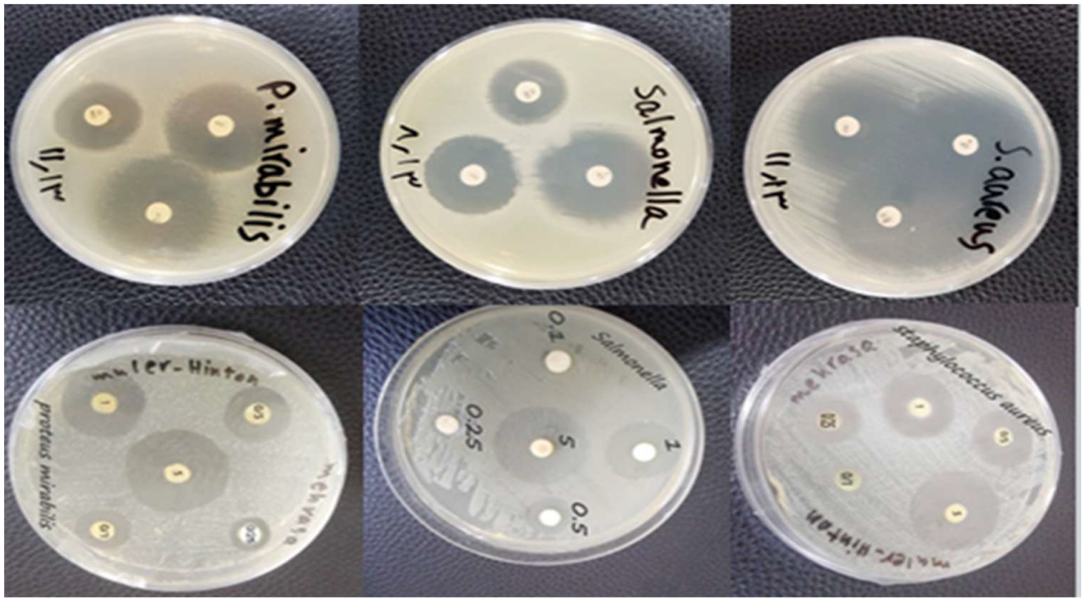

Figure 9: Diameter of the bacterial growth inhibition zones produced by synthesized AgNPs (A) and control antibiotics (B) against the tested bacteria.

2026, Vol. 2, Article ID. 2026.0025
https://doi.org/10.69709/SusProc.2026.105210

Table 3: Diameter of inhibition zones (mm) caused by different concentrations of AgNPs synthesized from *M. spicata* extract and by control antibiotics against tested Gram-positive and Gram-negative bacteria.

Bacterial Strains	Zone of Inhibition (mm)							
	Concentration (mg/mL)					Standard Control Antibiotics		
	5	1	0.5	0.25	1	Ciprofloxacin	Gentamicin	Sulfamethoxazole Trimethoprim
S. aureus ATCC 29213	14 ± 0.2^{a}	11 ± 0.1^{a}	9 ± 0.1^{b}	8 ± 0.1^{a}	6 ± 0.1^{a}	15 ± 0.3^{b}	15 ± 0.4^{a}	12 ± 0.2^{a}
Proteus mirabilis	13 ± 0.1^{b}	11 ± 0.2^{a}	9.3 ± 0.1^{a}	7.5 ± 0.2^{b}	3 ± 0.1^{b}	16 ± 0.4^{a}	9 ± 0.3^{b}	6 ± 0.1^{b}
S. typhimurium ATCC14028	12 ± 0.2^{c}	9 ± 0.2^{b}	7 ± 0.1^{c}	0^{c}	0^{c}	8 ± 0.1^{c}	7 ± 0.1^{c}	5 ± 0.1^{c}

Results are expressed as mean ± standard deviation (SD) (n = 3). Statistical analysis was performed using one-way analysis of variance (ANOVA) followed by Tukey's post hoc test in SPSS software. Differences were considered statistically significant at $p < 0.05$. Mean values in the same column with different superscript letters (a–c) indicate significant differences.

4. Conclusions

This study showed that *M. spicata,* a native plant of Mazandaran province, is a rich source of polyphenols. Its phenolic compounds were associated with antioxidant and other biological activities, with potential medicinal benefits. This study compared several extraction methods, including Soxhlet extraction, maceration, and ultrasonic-assisted extraction. At a solid-to-solvent ratio of 1:20 (g/mL), ultrasonic extraction showed the best efficiency. The IC50 value of the ultrasonic extract was 34.0217 µg/mL. Additionally, there were 106.22 mg GAE/g dry plant material. A color change from colorless to brown indicated the formation of AgNPs. The optimal synthesis conditions were established at pH 9.0, 60 °C, and an extract concentration of 1 g/L following the optimization of several parameters, including temperature, pH, extract concentration, and reaction time. XRD confirmed the structural properties of AgNPs. Phenolic compounds present in the *M. spicata* extract played a crucial role in the reduction of silver ions and stabilization of the nanoparticles, as indicated by FTIR analysis. SEM analysis further confirmed the successful synthesis of nanoparticles with an average particle size of 58.41 nm. Overall, the results demonstrate that the synthesized AgNPs exhibit effective antibacterial activity against both Gram-positive and Gram-negative bacterial strains.

5. Future Work

Nanoparticles synthesized using plant-based resources exhibit significant antibacterial and antioxidant properties, making them highly promising for a wide range of applications. Future work should focus on synthesizing nanoparticles using natural, commonly available edible materials [57–60] and medicinal plant roots, including *Rubia cordifolia* [61] and *Withania somnifera* [62], which have been reported in the literature to contain compounds with antimicrobial and antioxidant activities [57–63]. Nanoparticles prepared from such renewable resources can be applied as antimicrobial agents in pharmaceutical formulations and in wound dressings to promote healing and prevent infections. In addition, when derived from edible resources, they can be utilized in the development of innovative packaging materials for high-value food products with short shelf lives [64,65]. Furthermore, their biocompatibility and environmentally friendly synthesis process suggest potential applications in targeted drug delivery systems, biomedical devices, and cosmetics. Additionally, these nanoparticles may be explored as catalysts in chemical reactions and for environmental applications such as water purification. Such applications may contribute to economic development while supporting the achievement of the Sustainable Development Goals.

List of Abbreviations

AgNPs	Silver Nanoparticles
ATCC	American Type Culture Collection
DMSO	Dimethyl Sulfoxide
DPPH	2,2-Diphenyl-1-Picrylhydrazyl
FTIR	Fourier-Transform Infrared Spectroscopy
GAE	Gallic Acid Equivalents
IC_{50} (IC50)	Half-Maximal Inhibitory Concentration
M. spicata	*Mentha spicata*
P. mirabilis	*Proteus mirabilis*
S. aureus	*Staphylococcus aureus*
S. typhimurium	*Salmonella typhimurium*
SD	Standard Deviation
SEM	Scanning Electron microscopy
TPC	Total Phenolic Content
XRD	X-ray Diffraction

Author Contributions

Conceptualization, software, formal analysis, validation, writing—original draft preparation: S.M. and P.A.; Investigation, methodology, formal analysis, validation, writing—original draft preparation, writing—review and editing: S.M., P.A., M.Y.R., and M.E.; Visualization, funding acquisition: S.M., P.A., M.Y.R., and M.E.; Supervision, writing—review and editing: P.S.N. All authors have read and agreed to the published version of the manuscript.

Availability of Data and Materials

All data included in this study are available upon request.

Conflicts of Interest

The authors declare no conflicts of interest.

Funding

This research funding was granted to Mehrasa Yazdanpanah Rostami in the Department of Biotechnology at the Faculty of Chemical Engineering, Babol Noshirvani University of Technology, for research conducted by S. Mousavi, P. Ashooriyan, M. Y. Rostami, and M. Erfani. There is no grant number, this was supported by departmental internal resources.

Acknowledgments

The authors extend their appreciation to Babol Noshirvani University of Technology, Faculty of Chemical Engineering, for providing financial support for this project. The authors sincerely thank Dr. Morteza Hossieni (Department of Chemical Engineering, Babol Noshirvani University of Technology) for his valuable guidance throughout this research.

AI Declaration

The authors acknowledge the use of ChatGPT (OpenAI) solely for language editing and grammatical improvement of manuscript. The scientific content, data analysis, and interpretation of results were entirely conducted by the authors and they take full responsibility for the accuracy and integrity of the work.

References

[1] Alavi, M.; Kamarasu, P.; McClements, D.J.; Moore, M.D. Metal and Metal Oxide-Based Antiviral Nanoparticles: Properties, Mechanisms of Action, and Applications. *Adv. Colloid Interface Sci.* **2022**, *306*, 102726. [CrossRef]

[2] Tanwar, S.N.; Parauha, Y.R.; There, Y.; Swart, H.C.; Dhoble, S.J. Plant-Based Biosynthesis of Metal and Metal Oxide Nanoparticles: An Update on Antimicrobial and Anticancer Activity. *ChemBioEng Rev.* **2024**, *11*, e202400012. [CrossRef]

[3] Panwar, M.S.; Pal, P.; Joshi, D. Advances in Green Synthesis of Silver Nanoparticles: Sustainable Approaches and Applications. *J. Drug Deliv. Ther.* **2024**, *14*, 177–184. [CrossRef]

[4] Jeevanandam, J.; Kiew, S.F.; Boakye-Ansah, S.; Lau, S.Y.; Barhoum, A.; Danquah, M.K.; Rodrigues, J. Green Approaches for the Synthesis of Metal and Metal Oxide Nanoparticles Using Microbial and Plant Extracts. *Nanoscale* **2022**, *14*, 2534–2571. [CrossRef]

[5] Adelere, I.A.; Lateef, A. A Novel Approach to the Green Synthesis of Metallic Nanoparticles: The Use of Agro-Wastes, Enzymes, and Pigments. *Nanotechnol. Rev.* **2016**, *5*, 567–587. [CrossRef]

[6] Hussain, A.I.; Anwar, F.; Chatha, S.A.S.; Jabbar, A.; Mahboob, S.; Nigam, P.S. *Rosmarinus officinalis* Essential Oil: Antiproliferative, Antioxidant and Antibacterial Activities. *Braz. J. Microbiol.* **2010**, *41*, 1070–1078. [CrossRef]

[7] Hussain, A.I.; Anwar, F.; Nigam, P.; Ashraf, M.; Gilani, A.H. Seasonal Variation in Content, Chemical Composition and Antimicrobial and Cytotoxic Activities of Essential Oils from Four *Mentha* Species. *J. Sci. Food Agric.* **2010**, *90*, 1827–1836. [CrossRef] [PubMed]

[8] Silva, B.N.; Cadavez, V.; Caleja, C.; Pereira, E.; Calhelha, R.C.; Añibarro-Ortega, M.; Finimundy, T.; Kostić, M.; Soković, M.; Teixeira, J.A.; et al. Phytochemical Composition and Bioactive Potential of *Melissa officinalis* L., *Salvia officinalis* L. and *Mentha spicata* L. Extracts. *Foods* **2023**, *12*, 947. [CrossRef]

[9] Nouri, A.; Yaraki, M.T.; Lajevardi, A.; Rezaei, Z.; Ghorbanpour, M.; Tanzifi, M. Ultrasonic-Assisted Green Synthesis of Silver Nanoparticles Using *Mentha aquatica* Leaf Extract for Enhanced Antibacterial Properties and Catalytic Activity. *Colloid Interface Sci. Commun.* **2020**, *35*, 100252. [CrossRef]

[10] Ojewumi, M.E.; Adedokun, S.O.; Ayoola, A.A.; Taiwo, O.S. Evaluation of the Oil Extract from *Mentha spicata* and Its Chemical Constituents. *Int. J. Sci. Res.* **2018**, *74*, 68–89. [View Online]

[11] Thantry, A.D.K.; Chakravarthi, K.K.; Thundakattil, A.V.; Vasodavan, K. Traditional Aqueous and Ethanol Maceration of *Hamelia patens* Leaves: A Phytochemical and Pharmacological Exploration. *Ann. Afr. Med.* **2025**, *25*, 266–272. [CrossRef]

[12] Vanlalveni, C.; Lallianrawna, S.; Biswas, A.; Selvaraj, M.; Changmai, B.; Rokhum, S.L. Green Synthesis of Silver Nanoparticles Using Plant Extracts and Their Antimicrobial Activities: A Review of Recent Literature. *RSC Adv.* **2021**, *11*, 2804–2837. [CrossRef]

[13] Qaeed, M.A. Examining the Varied Concentrations of *Mentha spicata* and *Ocimum basilicum* Affect the Synthesis of AgNPs That Restrict the Development of Bacteria. *Saudi J. Biol. Sci.* **2024**, *31*, 103899. [CrossRef]

[14] El Badawy, A.M.; Luxton, T.P.; Silva, R.G.; Scheckel, K.G.; Suidan, M.T.; Tolaymat, T.M. Impact of Environmental Conditions (pH, Ionic Strength, and Electrolyte Type) on the Surface Charge and Aggregation of Silver Nanoparticles Suspensions. *Environ. Sci. Technol.* **2010**, *44*, 1260–1266. [CrossRef] [PubMed]

[15] Ansari, M.; Ahmed, S.; Abbasi, A.; Khan, M.T.; Subhan, M.; Bukhari, N.A.; Hatamleh, A.A.; Abdelsalam, N.R. Plant Mediated Fabrication of Silver Nanoparticles, Process Optimization, and Impact on Tomato Plant. *Sci. Rep.* **2023**, *13*, 18048. [CrossRef]

[16] Farooq, U.; Qureshi, A.K.; Noor, H.; Farhan, M.; Khan, M.E.; Hamed, O.A.; Bashiri, A.H.; Zakri, W. Plant Extract-Based Fabrication of Silver Nanoparticles and Their Effective Role in Antibacterial, Anticancer, and Water Treatment Applications. *Plants* **2023**, *12*, 2337. [CrossRef]

[17] Torres-Martínez, Y.; Arredondo-Espinoza, E.; Puente, C.; González-Santiago, O.; Pineda-Aguilar, N.; Balderas-Rentería, I.; López, I.; Ramírez-Cabrera, M.A. Synthesis of Silver Nanoparticles Using a *Mentha spicata* Extract and Evaluation of Its Anticancer and Cytotoxic Activity. *PeerJ* **2019**, *7*, e8142. [CrossRef] [PubMed]

[18] Umar, H.; Aliyu, M.R.; Ozsahin, D.U. Iron Oxide Nanoparticles Synthesized Using *Mentha spicata* Extract and Evaluation of Its Antibacterial, Cytotoxicity and Antimigratory Potential on Highly Metastatic Human Breast Cells. *Biomed. Phys. Eng. Express* **2024**, *10*, 035019. [CrossRef] [PubMed]

[19] Ramzan, M.; Abusalah, M.; Ahmed, N.; Yean, C.Y.; Zeshan, B. Green Synthesis and Characterization of Silver Nanoparticles Using *Zingiber officinale* Extracts to Investigate Their Antibacterial Potential. *Int. J. Nanomed.* **2024**, *19*, 13319–13338. [CrossRef]

[20] Annamalai, J.; Nallamuthu, T. Green Synthesis of Silver Nanoparticles: Characterization and Determination of Antibacterial Potency. *Appl. Nanosci.* **2016**, *6*, 259–265. [CrossRef]

[21] Ashooriyan, P.; Mohammadi, M.; Darzi, G.N.; Nikzad, M. Development of *Plantago ovata* Seed Mucilage and Xanthan Gum-Based Edible Coating with Prominent Optical and Barrier Properties. *Int. J. Biol. Macromol.* **2023**, *248*, 125938. [CrossRef]

[22] Hudzicki, J. Kirby-Bauer Disk Diffusion Susceptibility Test Protocol. *Am. Soc. Microbiol.* **2009**, *15*, 1–23. [View Online]

[23] Qaeed, M.A.; Hendi, A.; Thahe, A.A.; Al-Maaqar, S.M.; Osman, A.M.; Ismail, A.; Mindil, A.; Eid, A.A.; Aqlan, F.; Al-Nahari, E.G.; et al. Effect of Different Ratios of *Mentha spicata* Aqueous Solution Based on a Biosolvent on the Synthesis of AgNPs for Inhibiting Bacteria. *J. Nanomater.* **2023**, *2023*, 3599501. [CrossRef]

[24] Moosavy, M.-H.; de la Guardia, M.; Mokhtarzadeh, A.; Khatibi, S.A.; Hosseinzadeh, N.; Hajipour, N. Green Synthesis, Characterization, and Biological Evaluation of Gold and Silver Nanoparticles Using *Mentha spicata* Essential Oil. *Sci. Rep.* **2023**, *13*, 7230. [CrossRef]

[25] Calubaquib, M.A.M.; Delfin, E.F.; Merca, F.E.; Villegas, L.C.; Cruz, A.F.; Paterno, E.S. Biogenic Synthesis and Characterization of Silver Nanoparticles (AgNPs) Produced by Indigenous Microorganisms Isolated from Banana (*Musa* spp) Soils. *J. Exp. Biol. Agric. Sci.* **2023**, *11*, 105–118. [CrossRef]

[26] Flieger, J.; Franus, W.; Panek, R.; Szymańska-Chargot, M.; Flieger, W.; Flieger, M.; Kołodziej, P. Green Synthesis of Silver Nanoparticles Using Natural Extracts with Proven Antioxidant Activity. *Molecules* **2021**, *26*, 4986. [CrossRef]

[27] Chopade, B.; Ghosh, S.; Patil, S.; Ahire, M.; Kitture, R.; Jabgunde, A.; Kale, S.; Pardesi, K.; Cameotra, S.S.; Bellare, J.; et al. Synthesis of Silver Nanoparticles Using *Dioscorea bulbifera* Tuber Extract and Evaluation of Its Synergistic Potential in Combination with Antimicrobial Agents. *Int. J. Nanomed.* **2012**, *7*, 483–496. [CrossRef] [PubMed]

[28] Amaladhas, T.P.; Sivagami, S.; Devi, T.A.; Ananthi, N.; Velammal, S.P. Biogenic Synthesis of Silver Nanoparticles by Leaf Extract of *Cassia angustifolia*. *Adv. Nat. Sci. Nanosci. Nanotechnol.* **2012**, *3*, 045006. [CrossRef]

[29] Miranda, A.; Akpobolokemi, T.; Chung, E.; Ren, G.; Raimi-Abraham, B.T. pH Alteration in Plant-Mediated Green Synthesis and Its Resultant Impact on Antimicrobial Properties of Silver Nanoparticles (AgNPs). *Antibiotics* **2022**, *11*, 1592. [CrossRef]

[30] Kamarudin, D.; Hashim, N.A.; Ong, B.H.; Hassan, C.R.C.; Manaf, N.A. Synthesis of Silver Nanoparticles Stabilised by PVP for Polymeric Membrane Application: A Comparative Study. *Mater. Technol.* **2022**, *37*, 289–301. [CrossRef]

[31] Razali, Z.; Norrizah, J.; Abdullah, S. *Impact of Temperature and pH on Antioxidant Activity of Green Silver Nanoparticles Fabricated from Ananas comosus Peel Extracts*; IOP Publishing: Bristol, UK, 2022. Available online: https://ui.adsabs.harvard.edu/abs/2022E%26ES.1019a2006R/abstract.

[32] Liu, H.; Zhang, H.; Wang, J.; Wei, J. Effect of Temperature on the Size of Biosynthesized Silver Nanoparticle: Deep Insight into Microscopic Kinetics Analysis. *Arab. J. Chem.* **2020**, *13*, 1011–1019. [CrossRef]

[33] Kaur, R.; Avti, P.; Kumar, V.; Kumar, R. Effect of Various Synthesis Parameters on the Stability of Size Controlled Green Synthesis of Silver Nanoparticles. *Nano Express* **2021**, *2*, 020005. [CrossRef]

[34] Ibrahim, N.H.; Taha, G.M.; Hagaggi, N.S.A.; Moghazy, M.A. Green Synthesis of Silver Nanoparticles and Its Environmental Sensor Ability to Some Heavy Metals. *BMC Chem.* **2024**, *18*, 7. [CrossRef]

[35] Cao, W.; Huang, T.; Xu, X.-H.N.; Elsayed-Ali, H.E. Localized Surface Plasmon Resonance of Single Silver Nanoparticles Studied by Dark-Field Optical Microscopy and Spectroscopy. *J. Appl. Phys.* **2011**, *109*, 034310. [CrossRef] [PubMed]

[36] Paul, T.K.; Jalil, M.A.; Mondal, P.K.; Moniruzzaman; Alim, A.; Halder, K. Morphological Characterization of Bio-Mediated Silver Nanoparticles from *Azadirachta indica* (Neem) Leaf Extract. *SciEn Conf. Series: Eng.* **2025**, *2*, 25–30. [CrossRef]

[37] Zhan, Z.; Xu, R.; Mi, Y.; Zhao, H.; Lei, Y. Highly Controllable Surface Plasmon Resonance Property by Heights of Ordered Nanoparticle Arrays Fabricated via a Nonlithographic Route. *ACS Nano* **2015**, *9*, 4583–4590. [CrossRef]

[38] Chatterjee, A.; Singh, N.; Chanu, W.K.; Singh, C.B.; Nagaraj, V.A. Phytochemical Screening, Cytotoxicity Assessment and Evaluation of *in Vitro* Antiplasmodial and *in Vivo* Antimalarial Activities of *Mentha spicata* L. Methanolic Leaf Extract. *J. Ethnopharmacol.* **2022**, *298*, 115636. [CrossRef]

[39] El Menyiy, N.; Mrabti, H.N.; El Omari, N.; Bakili, A.E.; Bakrim, S.; Mekkaoui, M.; Balahbib, A.; Amiri-Ardekani, E.; Ullah, R.; Alqahtani, A.S.; et al. Medicinal Uses, Phytochemistry, Pharmacology, and Toxicology of *Mentha spicata*. *Evid. -Based Complement. Altern. Med.* **2022**, *2022*, 7990508. [CrossRef]

[40] Gwada, C.A.; Ndivhuwo, P.S.; Matshetshe, K.; Aradi, E.; Mdluli, P.; Moloto, N.; Otieno, F.; Airo, M. Phytochemical-Assisted Synthesis, Optimization, and Characterization of Silver Nanoparticles for Antimicrobial Activity. *RSC Adv.* **2025**, *15*, 14170–14181. [CrossRef]

[41] Khalid, Z.; Javed, A.; Alyas, T.; Shaheen, S.; Nazish, M.; Khalid, R.; Al Obaid, S.; Ansari, M.J.; Kamal, A. Biosynthesis, Structural Characterization of Silver Nanoparticles Synthesized Using an Eco-Friendly Method with *Mentha spicata* L. Extract and Their Antimicrobial Activity and Toxicological Risk Assessment. *Results Chem.* **2024**, *7*, 101487. [CrossRef]

[42] Mat Yusuf, S.N.A.; Che Mood, C.N.A.; Ahmad, N.H.; Mahboob, S.; Nigam, P.S. Optimization of Biogenic Synthesis of Silver Nanoparticles from Flavonoid-Rich *Clinacanthus nutans* Leaf and Stem Aqueous Extracts. *R. Soc. Open Sci.* **2020**, *7*, 200065. [CrossRef] [PubMed]

[43] Al-Zahrani, S.; Astudillo-Calderón, S.; Pintos, B.; Pérez-Urria, E.; Manzanera, J.A.; Martín, L.; Gomez-Garay, A. Role of Synthetic Plant Extracts on the Production of Silver-Derived Nanoparticles. *Plants* **2021**, *10*, 1671. [CrossRef] [PubMed]

[44] Mustapha, T.; Misni, N.; Ithnin, N.R.; Daskum, A.M.; Unyah, N.Z. A Review on Plants and Microorganisms Mediated Synthesis of Silver Nanoparticles, Role of Plants Metabolites and Applications. *Int. J. Environ. Res. Public Health* **2022**, *19*, 674. [CrossRef]

[45] Ali, H.; Azad, A.K.; Khan, K.A.; Rahman, O.; Chakma, U.; Kumer, A. Analysis of Crystallographic Structures and Properties of Silver Nanoparticles Synthesized Using PKL Extract and Nanoscale Characterization Techniques. *ACS Omega* **2023**, *8*, 28133–28142. [CrossRef]

[46] Erdman, N.; Bell, D.C.; Reichelt, R. Scanning Electron Microscopy. In *Springer Handbook of Microscopy*; Hawkes, P.W., Spence, J.C.H., Eds.; Springer International Publishing: Cham, Switzerland, 2019; pp. 229–318. [CrossRef]

[47] Nagilla, B.; Ajmeera, A.; Sultana, K.; Reddy, P.K. The Synthesis and Characterization of Mint Leaf (*Mentha spicata*) Biological Silver Nanoparticles and Their Impact on Rat's Motor Coordination and Cognition. *Int. J. Pharm. Sci. Nanotechnol.* **2024**, *17*. [CrossRef]

[48] Kaddour, A.; Amara, D.G.; Moussaoui, Y.; Chemsa, A.E.; Alia, Z.; Kamarchou, A. Total Phenolic and Flavonoid Contents of *Mentha spicata* Leaves Aqueous Extracts in Different Regions of Algeria and Their Antioxidant, and Antidiabetic Activities. *Trop. J. Pharm. Res.* **2022**, *21*, 1907–1913. [CrossRef]

[49] Brahmi, F.; Nury, T.; Debbabi, M.; Hadj-Ahmed, S.; Zarrouk, A.; Prost, M.; Madani, K.; Boulekbache-Makhlouf, L.; Lizard, G. Evaluation of Antioxidant, Anti-Inflammatory and Cytoprotective Properties of Ethanolic Mint Extracts from Algeria on 7-Ketocholesterol-Treated Murine RAW 264.7 Macrophages. *Antioxidants* **2018**, *7*, 184. [CrossRef]

[50] Jamous, R.M.; Abu-Zaitoun, S.Y.; Akkawi, R.J.; Ali-Shtayeh, M.S. Antiobesity and Antioxidant Potentials of Selected Palestinian Medicinal Plants. *Evid. -Based Complement. Altern. Med.* **2018**, *2018*, 8426752. [CrossRef]

[51] Andleeb, S.; Khan, H.; Nisar, T.; Latif, Z.; Raja, S.A.; Awan, U.A.; Maqbool, K.; Khurshid, S. Interactions of Chitosan-Coated Green Synthesized Silver Nanoparticles Using *Mentha spicata* and Standard Antibiotics against Bacterial Pathogens. *Curr. Pharm. Biotechnol.* **2023**, *24*, 203–212. [CrossRef]

[52] More, P.R.; Pandit, S.; De Filippis, A.; Franci, G.; Mijakovic, I.; Galdiero, M. Silver Nanoparticles: Bactericidal and Mechanistic Approach against Drug-Resistant Pathogens. *Microorganisms* **2023**, *11*, 369. [CrossRef]

[53] Hashim, N.; Bashi, A.M.; Jasim, A. Biosynthesis of Silver Nanoparticles by Mentha spicata Ethanolic Leaves Extract and Investigation the Antibacterial Activity. In *AIP Conference Proceedings*; AIP Publishing LLC: Melville, NY, USA, 2019. Available online: https://www.researchgate.net/publication/339140202_Biosynthesis_of_Silver_Nanoparticles_by_Mentha_Spicata_Ethanolic_Leaves_Extract_and_Investigation_the_Antibacterial_Activity.

[54] Abdullateef, A.; Unegbu, I.A.; Halilu, E.M. Green Synthesis of Silver Nanoparticles from *Mentha spicata* L. Aqueous Extract and Evaluation of Its Antioxidant, Antibacterial and Anticancer Activities. *Res. Sq. Checked Manuscriptchecked* **2023**. [CrossRef]

[55] Abalaka, M.E.; Akpor, O.B.; Osemwegie, O.O. Green Synthesis and Antibacterial Activities of Silver Nanoparticles against *Escherichia coli*, *Salmonella typhi*, *Pseudomonas aeruginosa* and *Staphylococcus aureus*. *Adv. Life Sci.* **2017**, *4*, 60–65. [View Online]

[56] Todorova, M.; Petrova, V.; Ranguelov, B.; Avdeev, G.; Velkova, L.; Atanasova-Vladimirova, S.; Pisareva, E.; Tankov, C.; Tomova, A.; Dolashki, A.; et al. Green Synthesis of Antimicrobial Silver Nanoparticles (AgNPs) from the Mucus of the Garden Snail *Cornu aspersum*. *Molecules* **2025**, *30*, 2150. [CrossRef]

[57] Bontzolis, C.; Plioni, I.; Dimitrellou, D.; Boura, K.; Kanellaki, M.; Nigam, P.S.; Koutinas, A. Isolation of Antimicrobial Compounds from Aniseed and Techno-Economic Feasibility Report for Industrial-Scale Application. *Int. J. Food Sci. Technol.* **2022**, *57*, 5155–5163. [CrossRef]

[58] Wan, H.C.; Sultana, B.; Nigam, P.; Owusu-Apenten, R.K. Comparison of Iron (III) Reducing Antioxidant Capacity (iRAC) and ABTS Radical Quenching Assays for Estimating Antioxidant Activity of Pomegranate. *Beverages* **2018**, *4*, 58. [CrossRef]

[59] Chan, Y.M.; Cheng, N.K.; Nigam, P.; Owusu-Apenten, R.K. Effect of pH on the Radical Quenching Capacity of Tea Infusions Using the ABTS●+ Assay. *J. Appl. Life Sci. Int.* **2016**, *6*, 1–8. [CrossRef]

[60] Cheung, T.; Nigam, P.; Owusu-Apenten, R.K. Antioxidant Activity of Curcumin and Neem (*Azadirachta indica*) Powders: Combination Studies with ALA Using MCF-7 Breast Cancer Cells. *J. Appl. Life Sci. Int.* **2016**, *4*, 1–12. [CrossRef]

[61] Barlow, R.; Barnes, D.; Campbell, A.; Nigam, P.S.; Owusu-Apenten, R. Antioxidant, Anticancer and Antimicrobial Effects of *Rubia cordifolia* Aqueous Root Extract. *J. Adv. Biol. Biotechnol.* **2016**, *5*, 6–14. [CrossRef]

[62] Barnes, D.A.; Barlow, R.; Nigam, P.; Owusu-Apenten, R. Antioxidant, Anticancer and Antibacterial Activity of *Withania somnifera* Aqueous Root Extract. *J. Adv. Biol. Biotechnol.* **2016**, *5*, 1–6. [CrossRef]

[63] Efstratiou, E.; Hussain, A.I.; Nigam, P.S.; Moore, J.E.; Ayub, M.A.; Rao, J.R. Antimicrobial Activity of *Callendula officinalis* Petal Extracts against Fungi, as Well as Gram-Negative and Gram-Positive Clinical Pathogens. *Complement. Ther. Clin. Pract.* **2012**, *18*, 173–176. [CrossRef] [PubMed]

[64] Francis, D.V.; Dahiya, D.; Kurup, S.; Gokhale, T.; Nigam, P.S. Advancing Sustainability Through Circular Economy, Emerging Technologies and Bibliometric Insights Towards Innovative Biodegradable Packaging for Dairy Products, Contributing to Sustainable Development Goal 9, 12, 13. *SCI Sustain.* **2025**, *1*, e70005. [CrossRef]

[65] Francis, D.V.; Dahiya, D.; Gokhale, T.; Nigam, P.S. Sustainable Packaging Materials for Fermented Probiotic Dairy or Non-Dairy Food and Beverage Products: Challenges and Innovations. *AIMS Microbiol.* **2024**, *10*, 320–339. [CrossRef] [PubMed]